

Design of a new Nd:YAG Thomson scattering system for MAST^{a)}

R. Scannell,^{1,b)} M. J. Walsh,¹ P. G. Carolan,¹ A. C. Darke,¹ M. R. Dunstan,¹
 R. B. Huxford,^{1,c)} G. McArdle,¹ D. Morgan,¹ G. Naylor,¹ T. O'Gorman,¹ S. Shibaev,¹
 N. Barratt,² K. J. Gibson,² G. J. Tallents,² and H. R. Wilson²
¹EURATOM/UKAEA Fusion Association, Culham Science Centre, Abingdon, Oxfordshire, OX14 3DB,
 United Kingdom
²Department of Physics, University of York, Heslington, York YO10 5DD, United Kingdom

(Presented 13 May 2008; received 9 May 2008; accepted 23 July 2008;
 published online 31 October 2008)

A new infrared Thomson scattering system has been designed for the MAST tokamak. The system will measure at 120 spatial points with ≈ 10 mm resolution across the plasma. Eight 30 Hz 1.6 J Nd:YAG lasers will be combined to produce a sampling rate of 240 Hz. The lasers will follow separate parallel beam paths to the MAST vessel. Scattered light will be collected at approximately $f/6$ over scattering angles ranging from 80° to 120° . The laser energy and lens size, relative to an existing 1.2 J $f/12$ system, greatly increases the number of scattered photons collected per unit length of laser beam. This is the third generation of this polychromator to be built and a number of modifications have been made to facilitate mass production and to improve performance. Detected scattered signals will be digitized at a rate of 1 GS/s by 8 bit analog to digital converters (ADCs). Data may be read out from the ADCs between laser pulses to allow for real-time analysis.

© 2008 American Institute of Physics. [DOI: 10.1063/1.2971971]

I. INTRODUCTION

A new 120 spatial point core Nd:YAG (yttrium aluminum garnet) Thomson scattering (TS) system replaces an existing 19 spatial point system described in Ref. 1. While the existing system uses a mixture of one and two spatial channels per polychromator, the new system will use one polychromator per spatial point. New collection optics, polychromators and digitizers are being produced. Four existing 50 Hz 1.2 J lasers have been converted to 30 Hz 1.6 J and will be combined with four new 30 Hz 1.6 J lasers. The resultant system will improve from producing 1.2 J at 200 Hz to 1.6 J at 240 Hz. An existing edge TS system, described in Ref. 2, that views the same lasers as the core Nd:YAG system will benefit from the improved laser repetition rate and increased energy, but will remain otherwise unchanged. An existing ruby laser TS system,³ which shares collection optics with the core Nd:YAG TS system, will be modified to use as much as possible of the extra light captured by the new collection lens.

The aim of this new system is to diagnose physics events such as magnetic islands, pellet injection, and sawteeth. The system is designed to measure at high spatial resolution and achieve low systematic and random errors. Measuring at low error is important for observing the change in gradient over a narrow region during magnetic islands. The use of fast bursts of laser pulses has already been demonstrated. Lasers have

been fired $5 \mu\text{s}$ apart to measure plasma filaments⁴ and $200 \mu\text{s}$ apart to measure pedestal evolution.⁵ The increase from four to eight lasers will allow longer bursts and more flexibility. Figure 1 shows the layout of the collection optics and lasers for the core and edge TS systems.

II. PHOTON BUDGET AND ÉTENDUE

The new system uses a similar polychromator design to the existing system, hence étendue must be conserved. Increasing the $f/\#$ of scattered light collection from $f/12$ to $f/6$ increases the solid angle of light collected by a factor of 4. The increase in collection solid angle is offset by a decrease in scattering length from two channels of scattering length 24 mm per polychromator to a single channel of scattering length ≈ 10 mm. An étendue budget, given in Table I, shows that the étendue for light collection in the plasma by both new and existing systems and étendue for light imaged into the polychromator are similar.

The change from two spatial points per polychromator to a single spatial point per polychromator doubles the number of collected photons per scattering length at constant polychromator étendue. Scattered light to plasma light ratio is also improved by a factor of 2 by changing to a single spatial point per polychromator. The increase in laser energy further improves the error achieved. An estimated photon budget for new and existing core TS systems is given in Table II. The new Nd:YAG system will collect ≈ 2900 photoelectrons/cm per 10^{19} as opposed to the existing system which collects ≈ 540 photoelectrons/cm per 10^{19} . The horizontal lines in Fig. 2(a) indicate the number of expected photoelectrons due to background light and APD noise. The background emission is calculated from plasma bremsstrahlung assuming

^{a)}Contributed paper, published as part of the Proceedings of the 17th Topical Conference on High-Temperature Plasma Diagnostics, Albuquerque, New Mexico, May 2008.

^{b)}Electronic mail: rory.scannell@ukaea.org.uk.

^{c)}Also at RBH Optics, Burgess Hill, West Sussex RH15 8HL, United Kingdom.

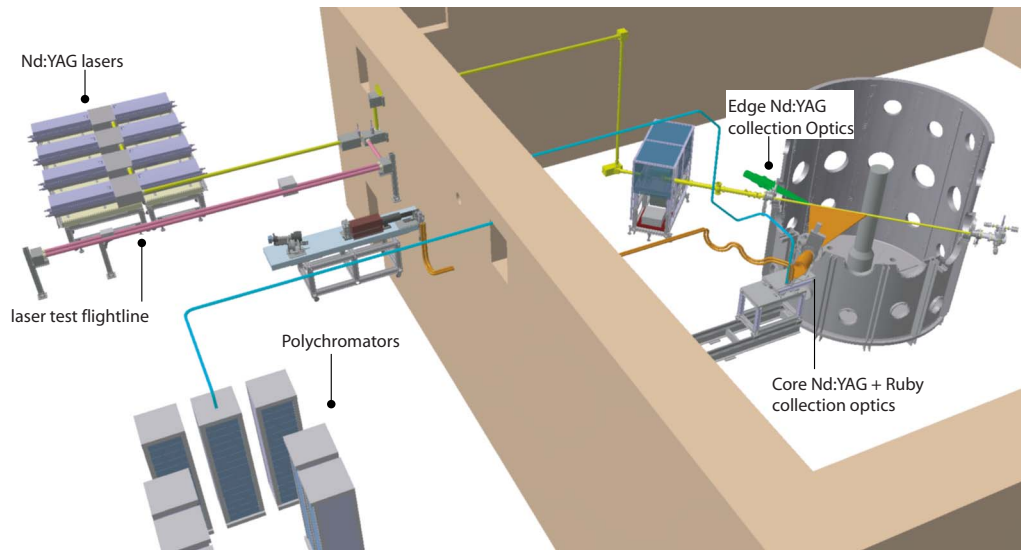


FIG. 1. (Color online) Layout of Nd:YAG system lasers and collection optics.

a flat plasma density profile of $2 \times 10^{19} \text{ m}^{-3}$ and a parabolic temperature profile of peak $T_e 2 \text{ keV}$. The calculated number of bremsstrahlung photoelectrons is increased by a factor of 4 to take into account other sources of background light such as line emission; this number of background photons is then reduced by a factor of 2 by use of a polarizer. The curved lines indicate the effective number of scattered photoelectrons received as a function of electron temperature in the spectral channels of a five spectral channel polychromator. From Fig. 2(a) the fractional error in T_e , n_e , and p_e is calculated and shown in Fig. 2(b). A wire grid polarizer described in Ref. 6 will be implemented in the collection optics to further reduce the background light.

III. POLYCHROMATOR DESIGN

This is the third generation of this Nd:YAG polychromator to be built. The first was designed for the core Nd:YAG system¹ and the second was for the edge system.² The main difference between the first and second generations was the changes to the optical interference filters to improve transmission in the passband region. This polychromator design has now been modified to facilitate easy manufacture.

The signal from each avalanche photodiode (APD) is electronically filtered by operational amplifiers by a high-pass (*fast*) channel and low-pass (*slow*) channel. The frequency response of these channels as well as the laser bandwidth are shown in Fig. 3. The fast channel is used to measure scattered signals of duration $\approx 10 \text{ ns}$. Signals below

TABLE I. Etendue budget for collection optics of new and existing systems and a polychromator.

	New	Existing	Polychromator
$\delta A \text{ (mm}^2\text{)}$	10×7	$24 \times 6 \times 2^a$	$\pi(3^2)/4$
$f/\#$	6	12	1.75
$\delta\Omega = \frac{\pi}{4f/\#^2} \text{ (sr)}$	0.0212	0.0055	0.256
$E = \delta A \delta\Omega \text{ (mm}^2 \text{ sr)}$	1.53	1.57	1.81

^aIn this system two spatial points are collected by a single polychromator.

$\approx 200 \text{ kHz}$ are removed, as fluctuations of this level are due to plasma events and digitizing slow varying light uses limited analog to digital converter (ADC) dynamic range. Since the laser bandwidth is $\approx 40 \text{ MHz}$, this high-pass filter has very little effect on the scattered light. ELMs on MAST have typical duration of $100 \mu\text{s}$ and so have a bandwidth of order 10 kHz . In existing polychromators the fast channel has successfully filtered out this slow varying light seen during ELMs and so there is little benefit in increasing the cutoff frequency of this channel. The slow channel is used to measure plasma background light and passes signals below 200 kHz . The photon statistical error on the measured scattered pulse is calculated from the sum of the number of photoelectrons in the scattered pulse and the background photoelectrons measured from the slow channel.

Previous polychromator designs had externally controllable gain in the polychromator electronics to magnify the amplitude of the signal from the APD. This circuitry has been removed since ADCs have variable input full scale ranges from 50 mV to 5 V . As may be seen from Fig. 2(a), the signal level in different spectral channels is different by a factor of 3 at constant electron density, primarily due to variation in detector quantum efficiency.

TABLE II. Photon budget for new and existing core TS systems.

	New Nd:YAG	Existing Nd:YAG	Ruby
Resolution (mm)	10	24	10
$f/\#$	6	12	15
Laser Energy (J)	1.6	1.2	10
EQE (%)	8–15	8–15	6.7
Transmission (%)	40	40	19
$f_{\text{detected}}^a \text{ (%)}$	60	60	90
(photoelectron/cm per 10^{19}) ^b	2900	540	1110

^aDetected fraction of photoelectrons at 1 keV .^bEffective number of detected photoelectrons per centimeter of scattering length per 10^{19} of plasma density. Note the existing Nd:YAG system has a scattering length of $2.5\text{--}4 \text{ cm}$.

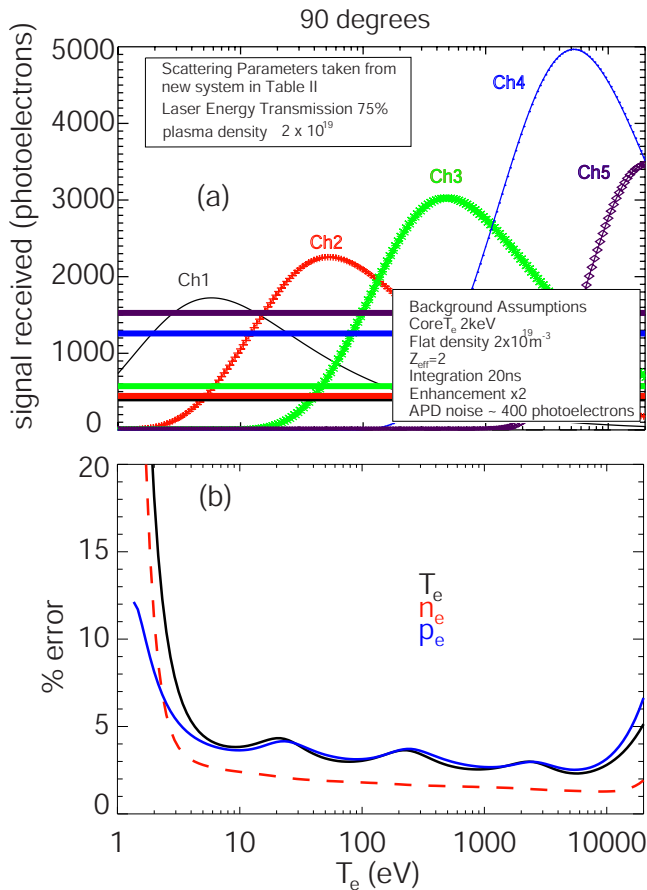


FIG. 2. (Color online) (a) The curved lines show scattered photoelectrons as a function of T_e . The horizontal lines show the expected numbers of background photoelectrons from a plasma with peak core T_e of 2 keV. (b) Fractional error as a function of electron temperature.

The APD gain is an increasing function of the APD reverse bias voltage. The APD gain is set to 250 kV/W at 25 °C in a reverse bias voltage specified by the manufacturer. The APD gain is a decreasing function of temperature.⁷ A thermal compensation circuit using a temperature sensitive diode inside the APD package has been designed so that the gain is constant over all temperatures.

The polychromator is designed to hold up to seven spectral channels, five of these are populated at present. The bandwidth of these spectral channels is designed to operate over a temperature range of 5 eV–10 keV. For a fixed temperature range, there is a design trade-off between the number of spectral channels and the flatness of the fractional

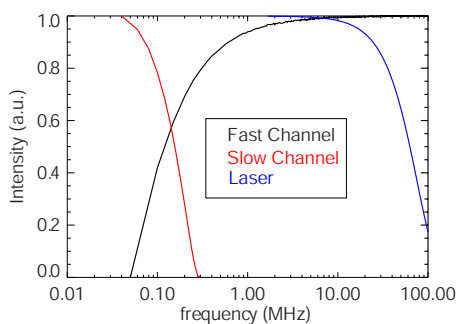


FIG. 3. (Color online) Frequency response of the fast and slow channels.

temperature error curve, shown in Fig. 2(b). The gaps between adjacent spectral channels are minimized to make best use of scattered photons.

IV. LASER SETUP

The eight lasers follow a parallel beam path of ≈ 25 m to the MAST vessel. The lasers are then imaged on to a lens which focuses the beams in the plasma. A typical damage threshold quoted for optics is 20 J/cm² for a 10 ns pulse at 1064 nm. For a pulse length of τ ns this scales as $(\tau/10)^{1/2}$ and so for a 6 ns pulse an expected estimate of 15.6 J/cm² is used. The 1.6 J laser pulse has a diameter of ≈ 2.5 cm at the vessel window and so has an energy loading of 0.32 J/cm², significantly below the damage threshold. This allows a margin of safety, as peaks of up to a factor of 4–5 in the laser intensity profile could be present. A software interlock is used to ensure all lasers cannot be fired simultaneously. The graphite beam dump is being replaced with a stainless steel dump with blades angled steeply to the direction of laser beam propagation to cope with the increased laser power. A laser test flight line in the laser room, shown in Fig. 1, replicates the laser beam path to the MAST vessel. This flight line is used to measure the beam profiles that will occur in the plasma.

V. COLLECTION OPTICS

Both refractive and reflective optic designs were considered for light collection. Due to the much larger size of the required mirror solutions a lens system was eventually chosen. The lens design has a stop aperture of 290 mm and collects at $f/6.0$ in the center of the plasma with a magnification of ≈ 0.29 to the $f/1.75$ fibers. The f number increases from the center of the plasma to $f/6.6$ at the outboard edge and $f/7.6$ at the inboard edge. The scattering length along the laser beam varies from 10 mm at the outboard edge to 12.7 mm at the inboard edge, radial resolution of < 10.5 mm is achieved everywhere. The eight parallel laser paths are staggered by up to 11 mm in the depth of field of the optics view. The collection optics design consists of six radiation tolerant lenses. The lenses are held in a collection cell of five separate elements. These elements will be combined as the lenses are inserted in the cell. The combined weight of collection cell and lenses is ≈ 90 kg, the cell has a diameter of 520 mm and length of 650 mm.

VI. POLYCHROMATOR SYSTEM LAYOUT

The polychromators and ADCs are housed in eight self-contained cubicles, one of which is shown in Fig. 4. Each cubicle contains 15 spectrometers and three compact PCI (cPCI) chassis. Each cPCI chassis contains up to eight cPCI cards and supplies up to 500 W of power to these cards. A hot-swappable redundant power supply stored in the chassis allows for easy replacement during operations.

The fast and slow signals from the spectrometers in each cubicle are digitized by ADCs contained in the three cPCI chassis. The fast ADCs digitize 8 bits at a rate of 1 GS/s and can store up to 2 Msamples of data per channel. Four digitizers are contained in a single cPCI card. Since a single

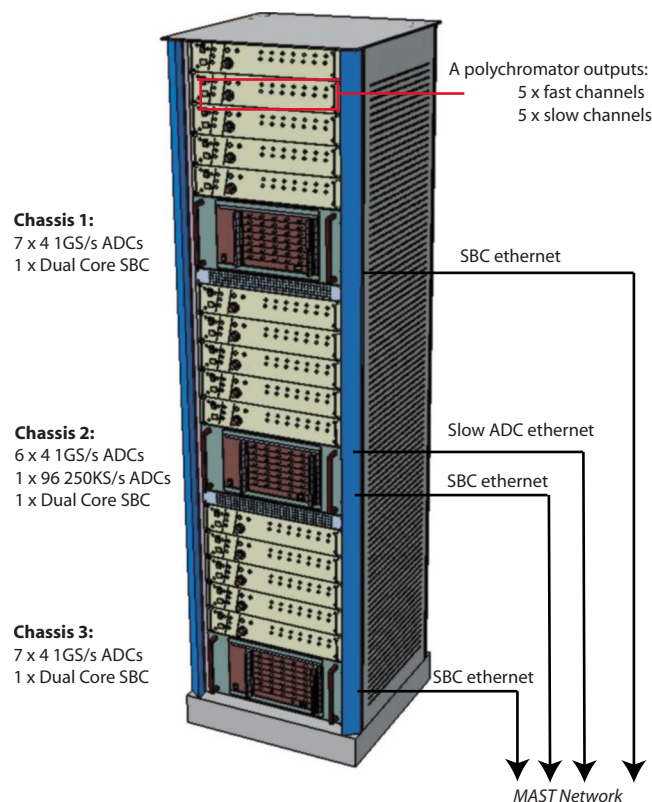


FIG. 4. (Color online) The layout of a cubicle containing 15 spectrometers and 3 cPCI chassis.

cubicle has 15 five channel polychromators, up to 19 ADC cards are required to digitize a single cubicle. The slow ADCs digitize at a rate of 250 KS/s with 16 bit resolution. A single slow ADC cPCI card can digitize up to 96 channels, and so provides for an entire cubicle of polychromators.

Data from the fast ADCs are read out to an embedded single board computer (SBC) housed in the same cPCI chassis. The embedded SBC then communicates with the network via an Ethernet hub. The embedded computer has a

high performance dual core Intel Xeon® processor and uses the server grade Intel E7520 and 6300ESB chipsets. The high performance CPU allows for potential real-time analysis. An ultralow voltage (ULV) processor was chosen to avoid potential overheating problems. In full-load operation running a windows operating system the ULV processor produces 39.5 W of power.

A single desktop control computer reads out the data from each of the individual SBCs and combines these data to create a single raw data file for each MAST shot. The same computer acts to control the ADC settings, voltage scale, samples per segment, number of segments, etc., for the ADCs housed in each chassis. The slow ADCs are separately networked and do not communicate with the SBC over the PCI bus.

ACKNOWLEDGMENTS

This work was funded jointly by the UK Engineering and Physical Sciences Research Council, EURATOM, the University of York and the Northern Way. We are indebted to the members of the TS project board and the Culham team, in particular, Alex Carter, Keith Hawkins, Steven Bailey, and Martin O'Brien, for their contributions.

- ¹M. J. Walsh, E. R. Arends, P. G. Carolan, M. R. Dunstan, M. J. Forrest, S. K. Nielsen, and R. O'Gorman, *Rev. Sci. Instrum.* **74**, 1663 (2003).
- ²R. Scannell, M. J. Walsh, P. G. Carolan, N. J. Conway, A. C. Darke, M. R. Dunstan, D. Hare, and S. L. Prunty, *Rev. Sci. Instrum.* **77**, 10E510 (2006).
- ³M. Walsh, N. J. Conway, M. Dunstan, M. Forrest, and R. B. Huxford, *Rev. Sci. Instrum.* **70**, 742 (1999).
- ⁴R. Scannell, A. Kirk, N. B. Ayed, P. G. Carolan, G. Cunningham, J. McCone, S. L. Prunty, and M. J. Walsh, *Plasma Phys. Controlled Fusion* **49**, 1431 (2007).
- ⁵A. Kirk, G. F. Counsell, G. Cunningham, J. Dowling, M. Dunstan, H. Meyer, M. Price, S. Saarelma, R. Scannell, M. Walsh, H. R. Wilson, and the MAST team, *Plasma Phys. Controlled Fusion* **49**, 1259 (2007).
- ⁶M. J. Walsh, P. G. Carolan, M. R. Dunstan, R. O'Gorman, and S. L. Prunty, *Rev. Sci. Instrum.* **75**, 3909 (2004).
- ⁷Characteristics and use of Si APD, Hamamatsu photonics K. K., Solid State Division, Catalog No. kapd9001e03, 2004.